

# EFFECTS ON DECENTRALIZED FEED-IN INTO DISTRICT HEATING NETWORKS – A SIMULATION STUDY

**Sven Paulick and Karin Rühling**

Institute of Power Engineering, Professorship of Building Energy Systems and Heat Supply,  
Technische Universität Dresden, Dresden, 01062, Germany, +49-351 / 463-34440, [sven.paulick@tu-dresden.de](mailto:sven.paulick@tu-dresden.de)

**Abstract** – The effects of decentralized feed-in into district heating (DH) networks are investigated as part of the research project “Prognose der Auswirkungen dezentraler Einbindung von Wärme aus erneuerbaren Energien und anderen Wärmeerzeugern in Fernwärmenetze” (*DELFIN*). The study focuses on the thermo-hydraulic impact with the resulting requirements for components like pumps, pressure maintenance, pipes as well as on the net control strategy. The aim is to identify allowed locations, the scale and temperature level for feed-in stations in terms of solar thermal or combined heat and power (CHP) technology. Furthermore, the necessity of heat storages and their operation mode as part of the network regulation is considered. Finally, conclusions will be made about the overall efficiency of the district heating network according to feed-in and operating mode.

## 1. INTRODUCTION

This paper presents the latest results of the research project “Prognose der Auswirkungen dezentraler Einbindung von Wärme aus erneuerbaren Energien und anderen Wärmeerzeugern in Fernwärmenetze”<sup>1</sup> and is based on the previous research project *DEZENTRAL* (Heymann, Rühling, Felsmann, 2017). The project partners are *Solites*<sup>2</sup> and *AGFW*<sup>3</sup>.

The results of the project *DEZENTRAL* have shown in detail, which effects can result with feed-in of decentralized heat into district heating networks. Flow reversal in part of the net branches, moving supply frontier or full supply of the decentralized producers can occur. The current project focusses on the impact in the network itself according to thermo-hydraulic effects and the consequent, alternating thermal stress of the pipes. Moreover, statements will be made about conditions when feed-in should be avoided according to network stability. Finally requirements for the feed-in pumps of the decentralized producers concerning to the location and local conditions in the network will be derived. A further aspect is the integration of a central thermal storage in the network. To prevent stagnation of installed solar thermal plants, the storage operation shall lead to a network load relief to decrease the stress in the network. Additionally, the following unloading can lead to a longer offline period of the central heat producer.

The simulation study focusses on two representative district heating networks with different structure and dimension to generalise the results for a wide field of application. The decentralized heat producers (DCP) are considered as solar thermal plants and combined heat and power units (CHP). A variation of decentralized heat producers according to size and position is part of the

investigation as well as different operation modes of the central heat storage. Combined with two different weather locations the simulation study will have a large spread of results to derive.

This paper presents the status of the simulation study as well as the realization of consumer, decentralized producer and storage modeling. The first simulation results of both networks are presented including first insights in the flow conditions. Furthermore, the integration of the storage in several operation modes will be discussed.

## 2. SIMULATION

### 2.1 Simulation Tools

The simulation study is realized by a coupling of two different simulation tools. For the thermo-hydraulic simulation of the district heating network, TRNSYS-TUD is used, as an in-house development on base of the Transient System Simulation Tool (TRNSYS). The advantage of TRNSYS-TUD is the developed thermo-hydraulic solver, adopted for the usage of district heating networks. It leads, especially for larger meshed networks, to adequate time taken for the simulation. The modeling of the consumer, decentralized heat producer and the storage is realized in the modeling language Modelica. The reason to choose Modelica as a second simulation tool is on the one hand the possibility to read in large MATLAB-Files and on the other hand diverse functionalities for dynamic simulation. The coupling of both simulation tools is realized with the Functional Mock-up Interface (FMI), a tool independent standard for co-simulation (Blochwitz, Otter, et al., 2011). The coupling works on a so-called Master-Slave-Technology. The models of the simulation tools represent the slaves, whereas the master controls the

<sup>1</sup> DELFIN: Founded by Federal Ministry for Economic Affairs an Energy (FKZ: 03ET1358B)

<sup>2</sup> Steinbeis Research Institute for Solar and Sustainable Thermal Energy Systems

<sup>3</sup> AGFW - Der Energieeffizienzverband für Wärme, Kälte und KWK e.V.

data exchange between the slaves between simulations time steps. Figure 1 shows the principle for the here mentioned simulation study. The used FMI-Master is an in-house development that enables the communication to TRNSYS-TUD.

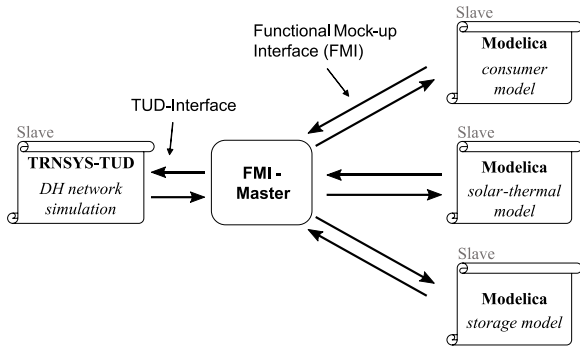


Figure 1: Schema of the coupling between TRNSYS-TUD and Modelica via FMI-Master

## 2.2 Considered District Heating Networks

Two different district heating networks are the research objects in the project. The first is a 3<sup>rd</sup> generation, radial DH network (following IEA-DHC Annex X classification), called Net G. The main characteristics are:

- installed load of 2.2 MW with a length of 2.65 km
- 51 consumers (in a range of 5.0 kW to 72.0 kW)

Up to five distributed decentralized heat producers (DCP) - in terms of solar thermal plants with each 100 m<sup>2</sup> gross area - are considered (compare Figure 2). A prospective integration of combined heat and power (CHP) units is planned.

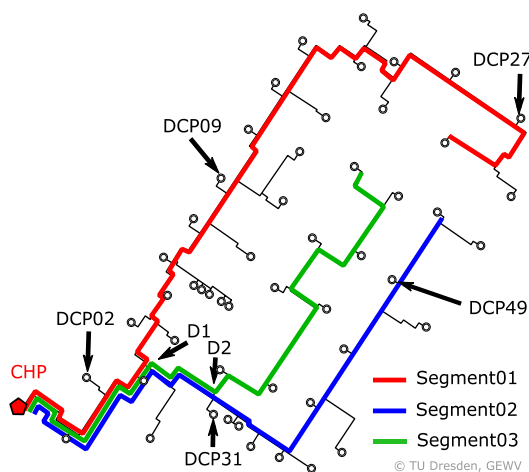


Figure 2: 3<sup>rd</sup> generation network - Net G - with central heat producer (CHP), segments and decentralized heat producer (DCP)

The second network is a 2<sup>nd</sup> generation, meshed DH network, called Net B, with the following main characteristics:

- installed load of 83 MW with a length of 41 km
- 485 consumers (in a range of 22 kW to 14.000 kW)
- four meshes
- further booster pump, installed in the return line

The simulation study focusses on the integration of up to 24 DCP in terms of solar thermal plants in this network. There are three different sizes of gross area installed with 500 m<sup>2</sup>, 1000 m<sup>2</sup> and 5000 m<sup>2</sup>, which are distributed in the network (compare Figure 3). The sizes correlate with the respective consumer at the location according to the installed load of  $\dot{Q}_{Ci} > 500 \text{ kW}$ ,  $> 1000 \text{ kW}$  and  $> 5000 \text{ kW}$ . Similar to Net G, decentralized CHP units will prospectively also considered.

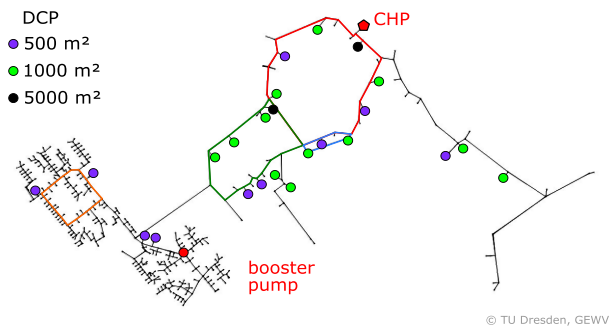


Figure 3: 2<sup>nd</sup> generation network - Net B - with central heat producer (CHP) and decentralized heat producer (DCP) according to size of collector gross area

The simulation study focusses on the two different weather data locations Würzburg and Potsdam (Germany), as regions with different radiation. The data source is *Deutscher Wetterdienst* (DWD), so original measured data is used for 2015. The reason is the possibly operation-mode for the CHP units according to EEX price-trend, which are combined with the respective weather data.

## 2.3 Principle of Consumer Modeling

Individual load profiles are crucial for a DH network simulation to prevent overestimated simultaneity in the network. The previous project *DEZENTRAL* used an adopted Typical-Day Method following VDI 4655 (2008). Measured data of consumer were adopted to specific weather data, and heat load profiles scaled to a given peak load. A detailed description can be found in (Heymann, Kretzschmar, Rosemann, Rühling, 2014).

However, this method was a pre-processing work and not suitable for larger DH networks, like Net B. Therefore, a new method was necessary that allows an online calculation of the heat load and return line temperature during the simulation. The developed procedure bases on linear regression models for 24 types of buildings (for

Net B) and two types of buildings for Net G. As data source, hourly measured data for heat load and return line temperature of one or two years as well as the respective weather data was considered. The data sources for the Net B are not from this original network, but from different unknown networks. This fact is a major advantage, because it allows using these regression models in several different DH network simulations.

As a first step, the identification of the major influencing parameters was done by regression analysis. The heat load of each building type  $\dot{Q}_{Ti}$  mainly depends on the outlet temperature  $\vartheta_o$ , the distinction of the working day  $W$  (equals one for working day, zero for a non-working day), the distinction of the heating period  $H$  (equals one for heating- and zero for non-heating period) and the hour of the day  $h$ , see equation (1).

$$\dot{Q}_{Ti} = f(\vartheta_o, \vartheta_o^2, W, H, h) \quad (1)$$

The return line temperature  $\vartheta_{RLi}$  of each building type additionally depends on the supply temperature at the consumer  $\vartheta_{SLi}$  as well as on the current heat load of the respective consumer  $\dot{Q}_{Ci}$ , see equation (2).

$$\vartheta_{RLi} = f(\vartheta_o, \vartheta_o^2, W, H, h, \vartheta_{SLi}, \dot{Q}_{Ci}) \quad (2)$$

As a result, a set of regression coefficients were derived for each building type dependent on the hour of the day  $h$  and the heating period  $H$ . During the simulation, in each time step the relevant regression coefficients are used together with the other influencing parameters to calculate the heat load and return line temperature of each building type. Finally, the heat load for each consumer  $\dot{Q}_{Ci}$  is scaled to the installed heat load of the connection point of the consumer.

The distribution of the different regression models in the network was realised, for example in Net B, by information of the network operator about the type of consumer (e.g. residential building, industry).

The validation of the DH network simulation with measured data of the network operator (at the central heat producer) has shown an adequate result. The principle of using regression models from measured data of unknown networks was successfully tested. In that case, the problem of overestimated simultaneity was not present after the implementation due to an advantageous distribution of the consumer models. However, in case of a higher simultaneity the regression models can easily be transformed regarding the heat load or time.

#### 2.4 Decentralized Heat Producer

As mentioned before, two types of decentralized heat producers (DCP) are considered – solar thermal plants and combined heat and power units. The peak load of the DCP depends according to network G or B and the location within.

The project partner *Solites* developed the model of the solar thermal plant. The model is implemented in an *EXCEL*-tool and contains the calculation of the insolation towards the inclined plane, the collector and the required components like heat exchanger and pipes. As an input, the supply and return line temperature at the feed-in point as well as the temperature setpoint is required. The possibly heat to the network is the result for each time step. For usage in a dynamic simulation, the model needed to be transferred into the modeling language Modelica for coupling with the network simulation of TRNSYS-TUD (see part 2.1).

All solar thermal plants in the simulation study have the following characteristics:

- 30° tilted collector
- southern orientation
- high-temperature flat plate collector
- water-glycol mixture
- target temperature equals setpoint reset curve of the network as  $f(\vartheta_o)$  plus additional offset due to heat exchanger
- feed-in point to the DH network just right before a consumer

The installed peak load leads with the respective installed collector gross area to the following total peak load (see Table 1).

Table 1: Overview of collector size and peak load

	coll.-area [m <sup>2</sup> ]	quantity	total coll.-area [m <sup>2</sup> ]	total peak-load [kW]
Net G	100	5	500	350
	500	10	5000	3500
Net B	1000	12	12000	8400
	5000	2	10000	7000
	$\Sigma$	24	27000	18900

The consequent ratio of the installed load of the network with the total peak-load of the installed solar thermal plants amounts to 15.9 % solar coverage for Net G, and 22.8 % solar coverage for Net B.

The integration of CHP units as the second category of decentralized heat producers is at the current state of the simulation study not yet implemented. It is planned to locate the CHP units just right before the consumers, similar to the solar thermal plants.

#### 2.4 Storage Integration

The integration of a heat storage can be an element to reduce the impact of decentralized feed-in heat in the DH network. If solar thermal plants are installed in the network, the aim is to get as much as possible heat into the

network. However, in times of highest solar heat gains, the heat demand in the network can be much lower. To prevent stagnation of the solar thermal plants in the network the integration of heat storages (central or decentral) can be one tool for net stabilisation and more effective operation. In this simulation study, one heat storage at the central heat producer is considered with different operation modes. The stagnation of all solar thermal plants installed is permitted, that means that an excess of heat in the network will directly load the storage. The heat storage is considered here only per energy balance sheet without thermal losses. As a first step, three storage operation modes (SO) were implemented, distinguished by the way of unloading:

- SO-P: permanent unloading allowed if necessary
- SO-D: daily unloading allowed between 8:00 PM and 8:00 AM if necessary
- SO-W: weekly unloading allowed between Friday 8:00 PM and Monday 8:00 AM

The loading of the storage is allowed at all times. For first investigations, the size is unlimited to get an overview of the required demand. Loading of the storage occurs when a flow reversal in the supply line at the central heat producer is present due to an excess of heat in the network. In that case, the heat into the storage  $\dot{Q}_{ST,in}$  is calculated with the net mass flow  $\dot{m}_{net}$  and the temperature difference of  $\vartheta_{SL}$  and  $\vartheta_{RL}$ , (compare Figure 4). The return line temperature  $\vartheta_{RL}$  is equal to the lower storage temperature  $\vartheta_{ST,l}$ . As it is an energy balance sheet only consideration, the lower storage temperature needed to be defined for that case. Therefore, the lower storage temperature  $\vartheta_{ST,l}$  was set to the mean temperature of the network return line between April and September, as the main operation time of the storage. This assumption leads to adequate results without considering complex storage modeling. For the heat into the storage  $\dot{Q}_{ST,in}$ , the following equation (3) applies:

$$\dot{Q}_{ST,in} = \dot{m}_{net} \cdot c_p \cdot (\vartheta_{SL} - \vartheta_{ST,l}) \quad (3)$$

Similar, in case of unloading the storage the heat flow outside  $\dot{Q}_{ST,out}$  is defined in equation (4):

$$\dot{Q}_{ST,out} = \dot{m}_{net} \cdot c_p \cdot (\vartheta_{ST,u} - \vartheta_{RL}) \quad (4)$$

The upper storage temperature  $\vartheta_{ST,u}$  has approximately the required temperature for the supply line  $\vartheta_{SL}$ . The simplified treatment of the heat storage is a sufficient method for investigations of required storage size and the effect of different storage operation modes. Prospective enhancements are conceivable regarding the consideration of heat losses and losses through convective mixing.

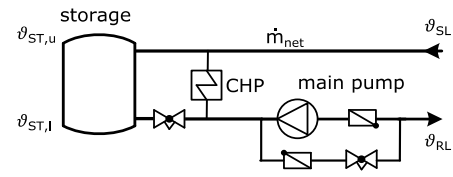


Figure 4: Heat storage integration at central heat producer (CHP)

### 3. RESULTS

The first representative results of the simulation are presented below. The analysis is done first via statistical evaluation of the annual simulation results by comparing the energy balances. Additionally the results of the storage operation modes will be treated. Finally the impact of decentralized feed-in to the network will be discussed on chosen examples.

#### 3.1 Feed-In Results

For both considered networks, first results for energy balances can be made, however at the current status of the project they are named preliminary.

The solar net fraction  $SF$  is defined as the ratio of the solar heat input by DCP  $\sum Q_{DCPi}$  to the sum of consumer demand  $\sum Q_{Ci}$  plus heat losses  $Q_{loss}$  of the network, see equation (5).

$$SF = \frac{\sum Q_{DCPi}}{\sum Q_{Ci} + Q_{loss}} \quad (5)$$

In Figure 5, the sum of DCP annual solar-thermal input  $\sum Q_{DCP}$  and the solar fraction  $SF$  are shown for the considered plants in both networks according to the location.

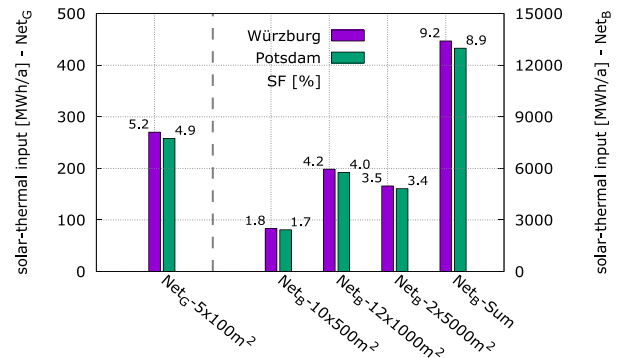


Figure 5: Solar-thermal input and solar fraction of all considered thermal plants acc. to location and network

In Net G, a solar fraction of around 5% was reached at both location. The specific annual solar-thermal input leads to 515 kWh/(m²·a) for Potsdam and 540 kWh/(m²·a) for Würzburg. The sum of the consumer demand  $\sum Q_{Ci}$  is 4893 MWh/a with losses of 304 MWh/a, for the example

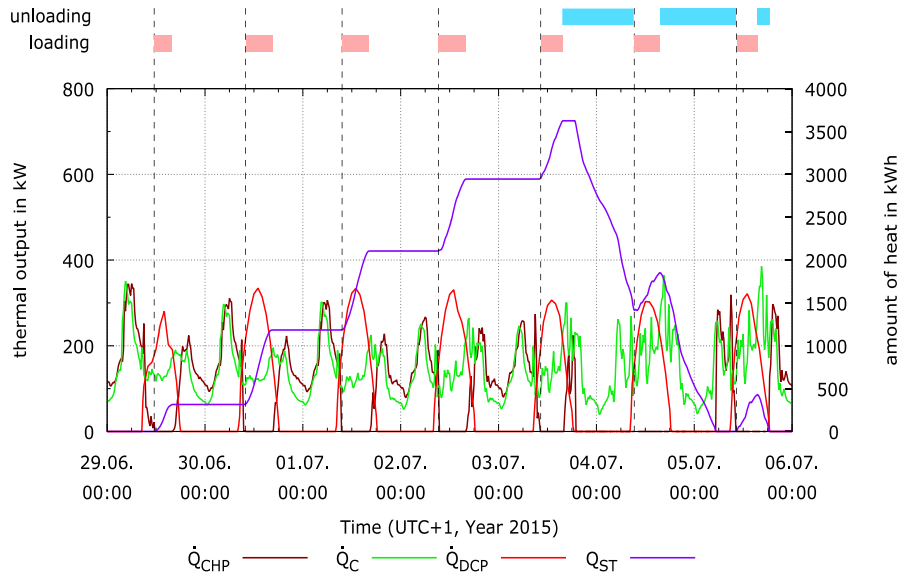


Figure 6: Example for weekly storage operation mode (SO-W) for Net G, Potsdam

of Würzburg. That means that the annual losses of the network are higher than the solar-thermal gains. For Net B, none of the variants with only one size of collector area reaches 5%. However, the heat load in the network is much higher. If all solar thermal plants are installed, almost 9% of solar fraction can be reached. The specific annual solar-thermal input leads to around 480 kWh/(m<sup>2</sup>·a) for Potsdam and around 497 kWh/(m<sup>2</sup>·a) for Würzburg. Here, the sum of the consumer demand  $\sum Q_{Ci}$  is 134419 MWh/a with losses of around 9191 MWh/a, considered variant *NetB-10x500m<sup>2</sup>* for example. In that case, the losses of the network are more than three times higher than the solar-thermal gains.

The first simulation results have shown that the amount and size of installed solar-thermal plants leads to a realistic solar fraction for existing networks. Moreover, the specific annual solar-thermal input is around 500 kWh/(m<sup>2</sup>·a), which stands for a high gain and makes it suitable for the investigations in this project regarding the thermo-hydraulic impact of feed-in.

### 3.2 Storage operation

A further focus of the simulation study is the integration of the heat storage with the mentioned operation modes. Currently Net G was successfully tested with storage operation and Net B is in progress.

The main parameters of interest here are the maximum required volume of the storage  $V_{ST,max}$  according to the operation mode as well as the sum of offline time of the central heat producer  $\sum h_{CHP,off}$ . In Table 2, the results are compared for Net G according to the operation mode for Würzburg. The results for Potsdam have slightly less sizes of  $V_{ST,max}$ , and are not mentioned here.

Table 2: Results of storage operation modes (Net G, Würzburg)

		SO-P	SO-D	SO-W
$V_{ST,max}$	[m <sup>3</sup> ]	38	38	98
$\sum h_{CHP,off}$	[h]	596	523	556
$\sum h_{DCP,in}$	[h]	1636	1636	1636

The required size of storage strongly depends on the operation mode. For the weekly mode, the maximum volume  $V_{ST,max}$  is around 2.5 times larger than for the other modes. As expected, the sizes for permanent and daily mode do not defer, because in both modes the unloading cannot reach the subsequent loading period to extend the necessary size. The comparison of the offline times of the central heat producer  $\sum h_{CHP,off}$  reveals that the highest value is not the mode with the highest storage size. Here, the time of unloading seems more relevant. This effect can be explained by the heat demand while unloading. Operation mode SO-D and SO-W allow unloading starting from 8:00 PM where the heat demand is commonly higher than in the afternoon. It leads, compared to SO-P, to a faster unloading with shorter offline time of the central heat producer. However, the amount of hours is just the sum without recognizing minimum operation and offline times of CHP. The heat input of all decentralized heat producers  $\sum h_{DCP,in}$  is at all storage operation modes equal, because of the same boundary conditions.

In Figure 6, the progress of weekly storage operation (SO-W) is presented with the amount of heat  $Q_{ST}$  in the storage, the overall consumer demand  $\dot{Q}_C$  and the heat input of the central  $\dot{Q}_{CHP}$  and decentral  $\dot{Q}_{DCP}$  heat producer. There are five loading periods during working days with the following unloading, starting on Friday at

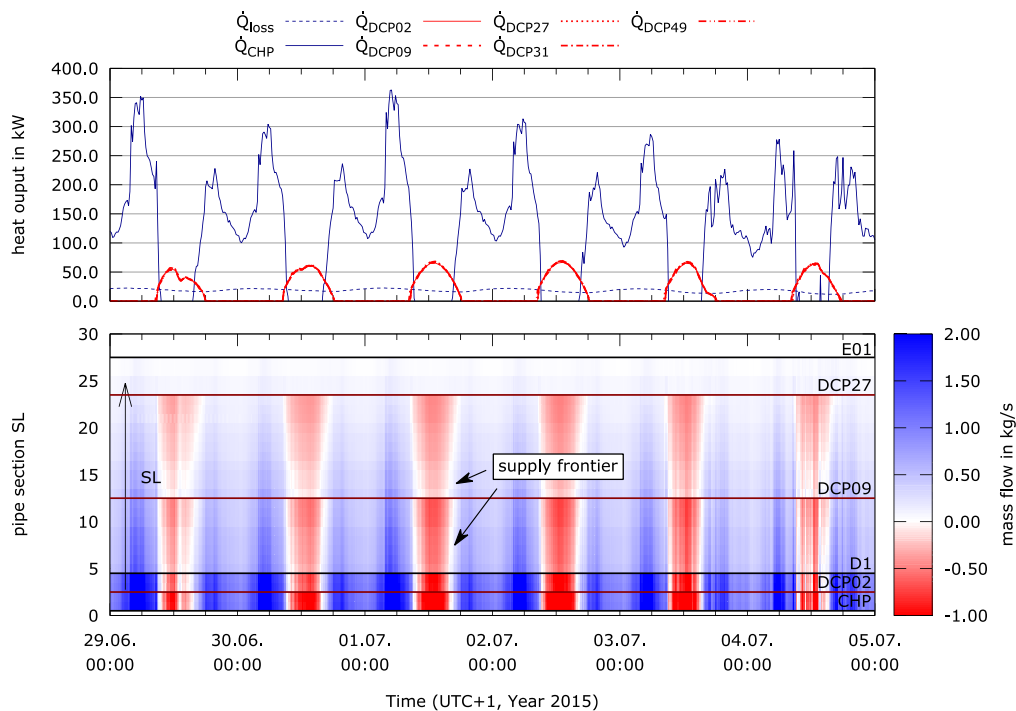


Figure 7: top: heat flow profiles, bottom: mass flow distribution; Net G, summer week, all DCP installed

8:00 PM. The loading of the storage is about a period of 103.25 h with a subsequent unloading about 34.75 h including a short reloading in between. That means that the central heat producer is offline for almost one and a half days, in case the maximum heat storage volume is installed.

### 3.3 Thermo-hydraulic Effects

The main aspect of the research project are the resulting effects of decentralized feed-in in the DH network. Therefore, the flow conditions needed to be investigated in detail. The following example presents the results of *Segment 01* of Net G (compare Figure 2). Similar analysis will be made for Net B, however simulations are currently ongoing.

Starting from the central heat producer, *Segment 01* has quite close the *DCP02*, followed by a network diversion *D1* and the further DCP's (*DCP09* and *DCP27*) till the end *E01*. Figure 7 (top) shows the progression of the heat flows for representative summer week. The heat load of the five decentralized heat producers in the network  $\dot{Q}_{DCP,i}$  proceed almost synchronous, because all of them have the same boundary conditions like collector type, tilt and installation. Smaller variations are caused by the slightly different temperatures at the feed-in point. The central heat producer is on every day for several hours offline, as seen in moments of  $\dot{Q}_{CHP} = 0 \text{ kW}$ . Here a full supply of the DCP's occurs in the network. The resulting effect of the network can be seen in Figure 7 (below). This time equivalent diagram shows distribution of the mass flow (in supply line) over the length of *Segment 01*. The red colour

indicates a flow reversal in the pipes due to an excess of heat in parts of the segment. The blue part with the different shades indicates fluctuations in the mass flow. The transition between both conditions is marked in white. The white zone indicates the supply frontier, where the flow velocity goes down to zero in this region (see the marked hint in Figure 7, below).

These alternating mass flow leads to alternating temperature profiles in the pipes. This is the main reason for thermal stress. Figure 8 shows the time equivalent temperature distribution of supply and return line. In the supply line, examples of supply frontier zones are marked. The temperature at these points is significant lower compare to the parts of feed-in, due to cool down of the stagnating flow. As the supply frontier is moving over time, an alternating thermal stress occurs at each pipe section. In the return line major fluctuations occur. During the night, the temperature is higher as a reaction of the consumer demand. The reaction of the moving supply frontier leads also to high fluctuation in the return line, to be seen as a shaded stream in the diagram along the line. Important to note is, that at the end of the return line (at the CHP) the temperature is almost homogenous. In the former project *DEZENTRAL*, high temperatures occur here in case of flow reversal. This was due to an installed bypass at the CHP instead of a storage, to use the network itself as short-term storage. The location had the highest thermal stress in the whole network. By installing the central heat storage at this point, the thermal stress might be reduced significantly. Further investigations to this topic will be part of the study in the near future.

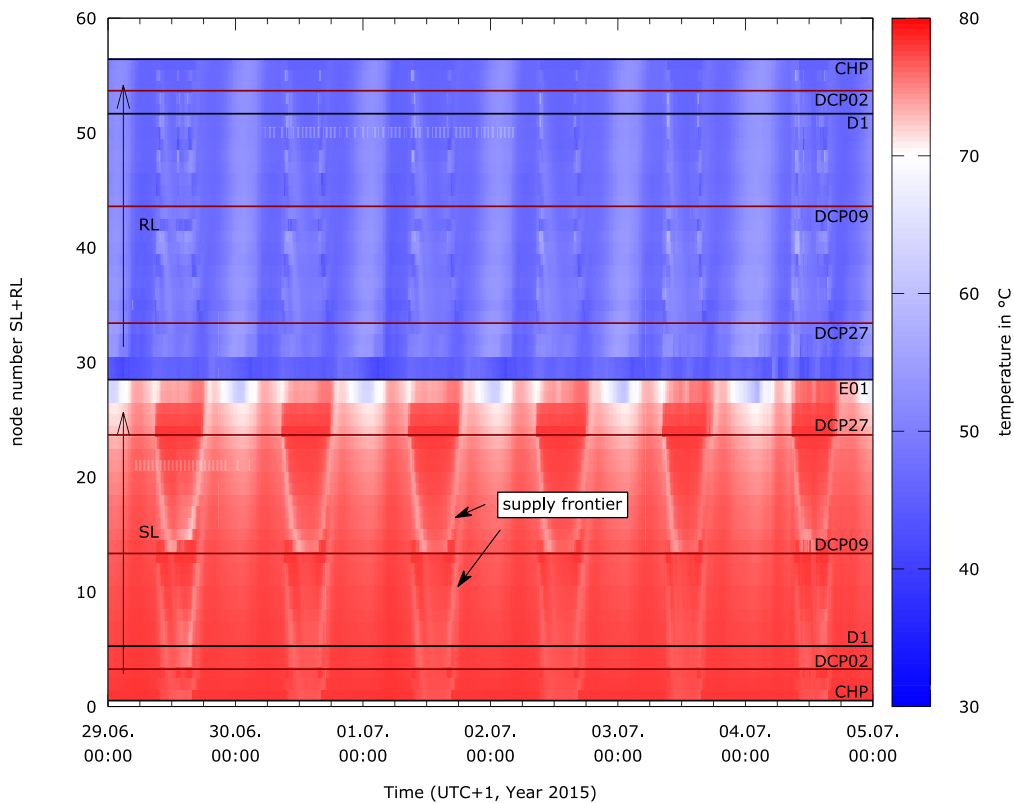


Figure 8: temperature distribution; Net G, summer week, all DCP installed

#### 4. CONCLUSION AND OUTLOOK

The realized *DELFIN* simulation studies shows further insights compared to the previous project *DEZENTRAL*. The developed principle of consumer modeling was tested successfully and validated with measurement data of the network operator. The selection and integration of the decentralized heat producers in terms of solar thermal plants has shown prospective relevant solar fraction rates for more renewable-based DH networks. Therefore, it can be the base for the following investigations. The study delivers first insights into the resulting operating conditions in the network and have shown a possibly reduction of thermal stress by integrating a central heat storage. However, this is a preliminary insight and further investigations are essential. The analysis of the heat storage integration has shown the necessity of distinction of various operation modes if energy efficiency is considered. However, finding an optimum between storage size, operation modes and possibly costs, will be interesting for the further investigations.

As a next step, the larger Net B with the four meshes and up to 9 % solar fraction will be considered in detail. Here the flow conditions in the mesh might change rapidly when large scale decentralized heat producer feeds in. Furthermore, the topic of thermal stress will be treated in

detail. Finally, the project will be derive requirements for pumps, pressure maintenance, pipes and net control strategy as a result of the investigated thermo-hydraulic effects.

#### NOMENCLATURE

##### Symbols

$h$	hour	h
$H$	heating period	0 / 1
$\dot{m}$	mass flow	kg/s
$Q$	heat	kWh
$\dot{Q}$	heat flow	W
$SF$	solar fraction	%
$V$	volume	m <sup>3</sup>
$W$	working day	0 / 1
$\vartheta$	celsius temperature	°C

## Abbreviations/Indices

C	consumer
CHP	central heat producer
DCP	decentralized heat producer
i, j	index
in	input / feed-in
l	lower
loss	losses
max	maximum
net	network
o	outlet
off	offline (out of operation)
out	output
RL	return line
SL	supply line
ST	heat storage
T	type
u	upper

## REFERENCES

- Blochwitz T., Otter M., Arnold M., Bausch C., Clauß C., Elmqvist H., Junghanns A., Mauss J., Monteiro M., Neidhold T., Neumerkel D., Olsson H., Peetz J.-V., Wolf S. (2011) *The Functional Mockup Interface for Tool independent Exchange of Simulation Models*, 8<sup>th</sup> International Modelica Conference 2011, Dresden
- Heymann M., Rühling K., Felsmann C. (2017) *Integration of Solar Thermal Systems into District Heating – DH System Simulation*, Energy Procedia, 116, Seoul doi:<https://doi.org/10.1016/j.egypro.2017.05.086>
- Heymann M., Kretzschmar T., Rosemann T., Rühling K. (2014) *Integration of Solar Thermal Systems into District Heating*, 2<sup>nd</sup> International Solar District Heating Conference, Hamburg